Chalcogenide Letters Vol. 13, No. 9, September 2016, p. 417 - 426

EFFECT OF HEAT TREATMENT ON THE STRUCTURAL MODIFICATION OF NEODYMIUM DOPED TELLURITE GLASS

N. A. M. JAN, M. R. SAHAR*
Advanced Optical Material Research Group, Department of Physics, Faculty of Science, Universiti Teknologi Malaysia, 81310 UTM Skudai, Johor, Malaysia.

Neodymium doped tellurite nanostructured glass having a composition of (75-x)TeO_2-15MgO-10Na_2O-(x)Nd_2O_3, where $0 \leq x \leq 2.5$ mol% has successfully been prepared by melt-quenching technique. The structure of crystallisation is determined using XRD technique and the existence of nanocrystalline nature of this glass is confirmed by TEM analyser. The physical properties of glass has been determined while their structural modification has been investigated using the IR and Raman spectroscopy analysis. The IR studies has shown that the structure of glass network consists of bending vibrations of Te-O-Te while, some structural units are TeO_4, TeO_{3+1}, and TeO_3 units.

(Received March 22, 2016; Accepted September 9, 2016)

Keywords: Tellurite glass, Neodymium, nanostructured glass, structural

1. Introduction

Tellurite glasses exhibit high non-linear refractive index compare to those of fluoride, phosphate and silicate glasses relatively. They also have good glass stability and highly corrosion resistance compare to those of fluoride glasses. Their low melting temperature and low phonon energy make them attractive hosts for active medium. TeO_2-based glasses with lower phonon energy could have higher quantum efficiencies and provide more fluorescent emissions than silica-based glasses. This implies that the tellurite glasses are suitable for nonlinear and laser applications.

The addition of glass modifier usually enhances the glass formation ability (GFA) in glass formers through the breaking chains of structural units. It will cause changes in structural formation units [1-4]. The structure of TeO_2 rich glasses have trigonal bipyramidal TeO_4, deformed TeO_4, TeO_{3+1} polyhedron and trigonal TeO_3 structural units. The network modifiers atoms can be easily attack two highly mobile axial bonds (Te-O_{ax}) in each TeO_4 unit. One of the Te-O_{ax} bonds in TeO_4 polyhedra elongates, the bond length increases and forms TeO_{3+1} structural unit when a network modifier like metal oxide is added into the glass matrix. Kaur *et al.* [5] reported that the subscript 3+1 indicates that the fourth oxygen is nearby but is not within a true bonding range. Structural unit of TeO_3 may be defined when the Te-O bond length exceeds the average length [6]. Addition, TeO_2 crystallizes in two different phases called α-TeO_2 (paratellurite, tetragonal) and β-TeO_2 (tellurite, orthorhombic) [3, 7] are known as stable phases. TeO_2 also form two metastable crystalline phases called γ-TeO2 (orthorhombic) and δ-TeO_2 (cubic) [8, 9].

In this study, the physical and structural properties are studied using XRD, FT-IR and Raman spectroscopy techniques on the samples of (75-x)TeO_2-15MgO-10Na_2O-(x)Nd_2O_3 glasses.

2. Experimental

The prepared glasses have a nominal composition of (75-x)TeO_2-15MgO-10Na_2O-(x)Nd_2O_3 with x in the range of $0 \leq x \leq 2.5$ mol%. The required proportion of TeO_2, MgO, Na_2O

*Corresponding author: mrahim057@gmail.com

and Nd_2O_3 powder and weighed separately using a sensitive balancing machine (Electronic Balance Precise 205A SCS ± 0.001 g). Then, the batch is carefully mixed in platinum crucible and milled for about 30 minutes to make sure the homogeneity of the mixing material.

The glass samples are prepared by the conventional melt-quenching methods. The batch is heated at 900°C for at least 30 minutes and the glass compositions are summarized in Table 1. Then, the molten is poured onto a preheated mould made of brass plate. After that, it is annealed at 300°C for 2 hours to remove the internal stress before allowed to slowly cool down to room temperature. The nanocrystals are grown by heat treatment to the selected glasses (TMN1, TMN3, and TMN6) at their respective T_c for 30 minutes.

Table 1: The glass composition (mol%) and their codes

Sample No.	Nominal composition (mol%)				Remarks
	TeO_2	MgO	Na_2O	Nd_2O_3	
TMN1	75.0	15.0	10.0	0.0	Heat treated at 30 min
TMN2	74.5	15.0	10.0	0.5	-
TMN3	74.0	15.0	10.0	1.0	Heat treated at 30 min
TMN4	73.5	15.0	10.0	1.5	-
TMN5	73.0	15.0	10.0	2.0	-
TMN6	72.5	15.0	10.0	2.5	Heat treated at 30 min

The density of the glass samples was determined by Archimedes principle.

$$\rho = \frac{W_a}{W_a - W_b}(\rho_x) \tag{1}$$

where W_a is the weight of the glass sample in air and W_b is the weight of the sample when immersed in distilled water. The (ρ_x) is density of distilled water 0.9975 gcm^{-1}. Molar volume of the glasses was calculated by using the equation:

$$V_M = \frac{M}{\rho} \tag{2}$$

where M is the molecular weight of glass formula unit and ρ is the density of glass.
The ionic packing density, V_t (in mol^3/mol) can be calculated by using:

$$V_t = \left(\frac{1}{V_M}\right)\sum(V_i x_i) \tag{3}$$

Where V_m is molar volume and x_i is molar fraction (in mol%).

$$V_i = \left(\frac{4\pi N_A}{3}\right)\left[X r_M{}^3 + Y r_o{}^3\right] \tag{4}$$

Where N_A is Avogadro's number (in mol^{-1}), r_M and r_o are the Shannon's ionic radius of metal and oxygen [10].

The X-ray diffraction (XRD) measurement is carried out to identify the amorphous nature of glass by using CuKα radiation operating at 40 kV, 30 mA using Siemens Diffractrometer D5000.

All infrared spectra of the glasses are recorded using a Perkin-Elmer Spectrum One FT-IR spectrometer over the range of wave number 4000–400 cm^{-1} at room temperature using 10 scans

at 4 cm^{-1} resolutions. A series of absorption peaks can be observed which reflect the vibration of the atoms at the IR region.

The Raman spectra are measured using a confocal Horbia Jobin Yvon (model HR800 UV) Raman spectrometer in the spectral range 200–2000 cm^{-1}, with the laser power on the samples being 1000 mW.

TEM analyser is performed to determine the size and shape of nanostructured glass. The nanocrystal of Neodymium doped tellurite glass is observed under the transmission electron microscope (TEM 2100, JEOL) with an acceleration voltage 200kV.

3. Results and discussion

3.1 XRD

Figure 1 shows the x-ray diffraction pattern of TMN6 sample before and after heat-treated. From Figure 1, it can be seen that there are no sharp peaks observed from the diffraction pattern. Thus, it can confirm that all prepared samples are amorphous in nature. From this figure, it can be seen that for the heat-treated sample, the glass is still dominated by the amorphous structure and the peak is related to nanocrystalline structures which are too small to be detected.

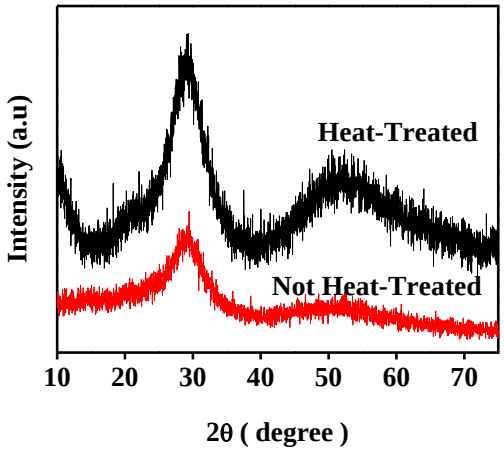

Fig. 1: X-ray diffraction patterns of glass samples.

3.2 Density, Molar Volume and Ionic Packing Density

A plot of density and molar volume against Nd concentration can be seen in Figure 2 (a) for as prepared glass sample and (b) for heat-treated glass sample (listed in Table 2). The density is increased while the molar volume is decreased with the increasing concentration of Nd. This might be related to the molecular weight of TeO_2 (atomic mass = 159.60 g/mol) is replaced by a higher molecular weight Nd_2O_3 (336.48). As the density is increased in the glasses studied, the glass network rigidity is increasing and free volume decreases in glass structure. Hence, the molar volume is decreased which is compliance with increment of T_g [11]. Therefore, the increase in density and decrease in molar volume shows the increment in glass compactness. This result is in agreement in other finding [12-14].

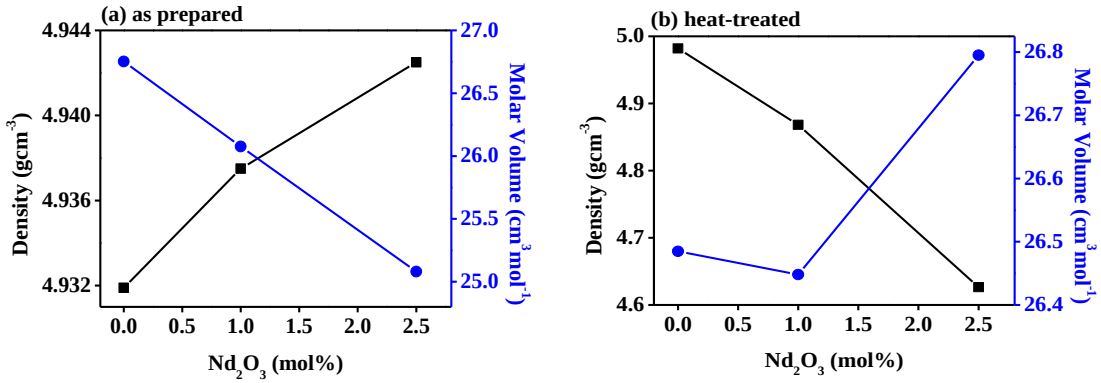

Fig. 2: The dependences of density and molar volume on the Nd_2O_3 concentration for (a) as prepared and (b) heat-treated samples.

Table 2: Physical properties of prepared samples.

Nd_2O_3 concentration (mol%)	As prepared			Heat-treated		
	Density (gcm^{-3})	Molar volume (cm^3mol^{-1})	Ionic packing density	Density (gcm^{-3})	Molar volume (cm^3mol^{-1})	Ionic packing density
0.0	4.9319	26.7530	0.4858	4.9819	26.4849	0.4907
1.0	4.9375	26.0767	0.5037	4.8681	26.4481	0.4966
2.5	4.9425	25.0813	0.5319	4.6264	26.7952	0.4979

Figure 3 shows the variation of ionic packing density with Nd_2O_3 concentration for as prepared and heat-treated glass sample. The result of ionic packing density is summarized in Table 2. The ionic packing density increases with the increase of Nd_2O_3 content. This is perhaps due to the dependence of density on the ionic radii of atom. Yusoff has been reported that larger the ionic radius, the chance that ions fit the space of excess volume is become higher [13]. Based on revision by Shannon [10], the ionic radius of Nd^{3+} is larger than the others substance (Te^{4+}, Mg^{2+}, Na^{1+}). As result, Nd ions have entirely filled the space and make the glass more compact.

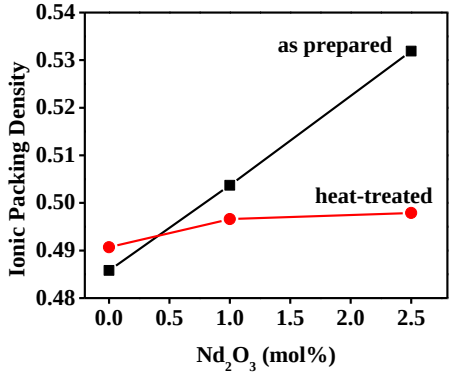

Fig. 3: Ionic packing density versus different Nd_2O_3 concentration on as prepared and heat-treated samples.

3.3 Transmission Electron Microscopy (TEM)

The size and morphology of the nanostructured glass is also investigated by transmission electron microscopy (TEM). Heat treatment causes crystallization of the matrix glass by inducing nucleation and crystal growth. Figure 4 shows the TEM image of the TMN6 sample after heat-treated at around 419℃ for 30 minutes. It is found that some of crystallite particles are spherical in

shape clearly visible as dark spots and are homogeneously dispersed in the amorphous tellurite network.

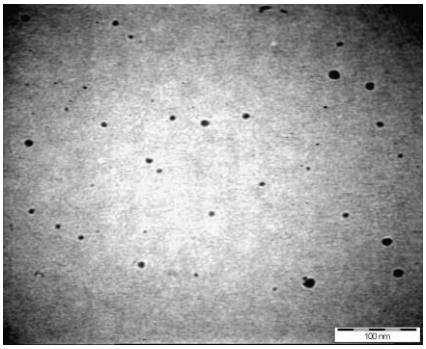

Fig. 4: TEM micrograph obtained of the heat treated TMN6 glass.

Heat treatment causes crystallization of the matrix glass by inducing nucleation and crystal growth. Then crystal particles can successfully precipitated in the glass matrix after thermal treatment. The frequency average size of crystal particles is ~8.3 nm by using Gaussian fit. It shows that the nanocrystals are used distributed in the glass matrix.

3.4 Fourier Transform Infra Red Spectroscopy

The information on the structure of the tellurite doped with Nd^{3+} ion can be obtained by using the Fourier Transform Infra Red (FTIR) technique. The FTIR spectra of the glasses are presented in Figure 5(a). The observed absorption peaks positions are presented in Table 3. The broad, strong and weak absorption bands can be seen in the investigated wave number 4000 - 400 cm^{-1}.

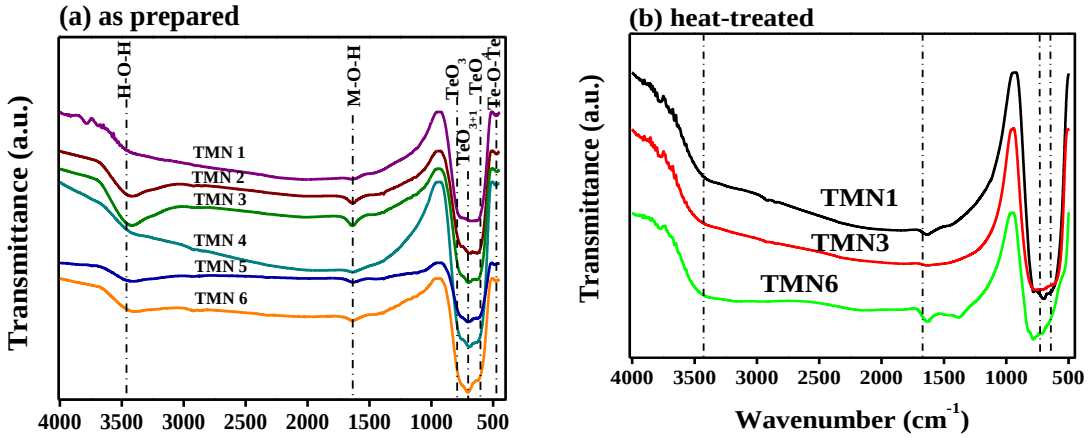

Fig. 5: FTIR spectra of (75-x)TeO_2-15MgO-10Na_2O-xNd_2O_3 (a) in the as-cast condition glass system with 0.0 ≤ x ≤ 2.5 mol% and (b) heat treated glass system with x= 0.0, 1.0 and 2.5 mol%.

Table 3: IR peaks positions for (75-x)TeO_2-15MgO-10Na_2O-xNd_2O_3 glass system where 0.0 ≤ x ≤ 2.5 mol%.

Nd_2O_3 concentration (mol%)	IR Peak Positions (cm^{-1})				
	Te-O-Te (Bending vibration)	TeO_4 (Stretching vibration)	TeO_3 (Bending vibration)	M-O-H (Bending vibration)	OH^- (Stretching vibration)
0.0	470	621	774	1637	3466
0.5	471	622	775	1630	3418
1.0	467	624	760	1634	3422
1.5	473	624	761	1625	3453
2.0	474	624	755	1636	3438
2.5	474	623	753	1628	3419

The spectra of the glasses presented in this work showed five bands. The bands appear around 467 - 474 cm^{-1} is assigned the bending mode of Te-O-Te or O-Te-O linkages [15]. The presence of continuous network consisting of TeO_n (n = 4, 3+1, 3) polyhedral is indicated by the existence of this peak. All small peaks arise by reason of the deformation of the Te-O bond vibration [16].

The trigonal pyramidal (tp) TeO_3 and bipyramidal (tbp) TeO_4 are the two structures of tellurium that built the glass network. Hu Z. [17] also reported that this broad peak ascribed to the mixing structures of TeO_3 groups, symmetric TeO_4 groups and deformed TeO_4 groups. In general case, the absorption of TeO_3 group has higher frequency position than TeO_4 [18]. Therefore, the band around 620 - 624 cm^{-1} attributes TeO_4 while the band range of TeO_3 correlates with frequency 783 - 828 cm^{-1}. The band shifts show some changes in the composition of the glass system as listed in Table 4. At 1.0 mol% Nd_2O_3, the band shifted to lower wavenumber which might be due to some of [TeO_{3+1}] polyhedral or [TeO_3] tp convert back to [TeO_4] tbp unit [19]. It can also be confirmed in Figure 6(a) when the band around 621 cm^{-1} is shifted to higher wavenumber which shows the increasing of TeO_4 content. The peak around 624 cm^{-1} has finally shifted to 623 cm^{-1} as the Nd_2O_3 content is increased up to 2.5 mol%. This shift could be indicated to the co-existence of the deformation of the TeO_4 group, whereas the band around 760 cm^{-1} is found shifted to 753 cm^{-1} which might be due to the formation of TeO_3 group. It is proposed that the transition of TeO_4 tbp unit to the TeO_3 tp through the formation of intermediate coordination of TeO_{3+1} [20, 21]. Thus, there is a change in the content of [TeO_{3+1}] structural units and non-bridging oxygen (NBO) in the glass network.

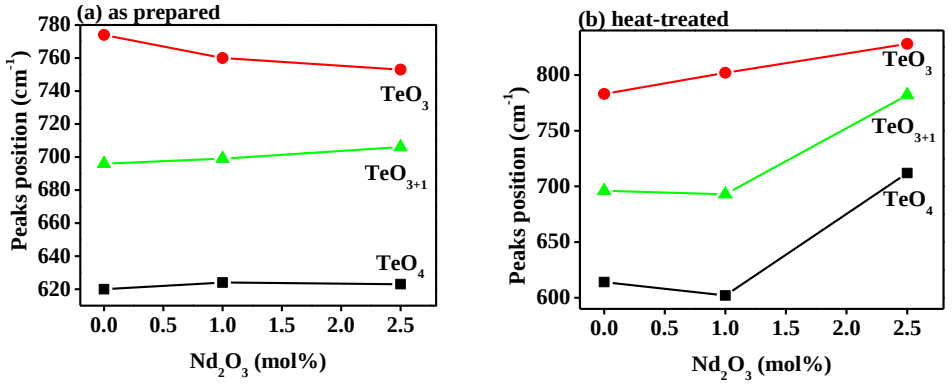

Fig. 6: IR peak positions of (a) as prepared and (b) heat-treated glass system.

Table 4: Comparison of IR peaks positions between as prepared and heat-treated glass.

Nd_2O_3 concentration (mol%)	IR Peak Positions (cm^{-1})					
	As prepared			Heat-treated		
	TeO_4	TeO_{3+1}	TeO_3	TeO_4	TeO_{3+1}	TeO_3
0.0	621	697	774	614	696	783
1.0	624	699	760	602	693	802
2.5	623	706	753	712	782	828

The OH group in the glass can be regarded as the ingredient of the glass because it is a kind of impurities in the host. The peak of this group is observed at the bands around 1600 cm^{-1} and 3400 cm^{-1} which are ascribed to the vibrations of water molecule and fundamental stretching of OH group respectively [22].

Figure 5(b) presents the FTIR spectra of the heat treated glass containing 0.0, 1.0, and 2.5 mol% Nd_2O_3. The spectra of the heat treated glasses show two bands near at 714 cm^{-1} and 780 cm^{-1} assigned to $v_{TeO_{2eq}}^{as}$ and $v_{TeO_{2eq}}^{s}$ respectively which are categorized the stretching frequencies in the IR spectrum of crystalline TeO_2 [23]. These bands are broadened relating to the crystalline TeO_2 because of the allocation of lengths and bond angles in the amorphous medium [24]. The TeO_3 groups developed the Te-O vibrations of crystalline tellurites possibly examined. In addition, the vibrations of tellurites and of α-TeO_2 built up by TeO_4 groups may be examined. For comparison, the structural units and of the short-range order, they are similar to the spectra of the crystalline phases [25]. This is again support the existence of nanocrystalline phase of α-TeO_2 in the glass system.

Generally, it seems that the band has shifted to a higher wavenumber by increasing Nd_2O_3 contents as can be seen in Figure 6(b) and listed in Table 4. At 1.0 mol% Nd_2O_3, the peak around 602, 693 and 802 cm^{-1} are shifted towards higher wavenumber whereas corresponding to the stretching vibrations of TeO_4 units, TeO_{3+1} and TeO_3 respectively. The shifting of this bands might be caused of the conversion process from TeO_4 to TeO_3 or TeO_{3+1} and formed (NBO) in the glass network [26].

The occurrence of the bands around 1600 cm^{-1} and 3400 cm^{-1}which assigned to the OH vibration band for heat treated glass is decreased compared with the before heat treatment glass. The reduction of OH can minimized the optical loss of a fiber assess which contribute to the decrease of the background loss.

3.5 Raman Spectroscopy

Figure 7(a) and (b) presents the $72.5TeO_2$-$15MgO$-$10Na_2O$-$2.5Nd_2O_3$ glass and the Raman spectrum of the crystalline respectively. Comparison of the peaks are shifted in the peak position and changed in the width might be because of the effect of heat treatment. The Raman spectra in Figure 7(a) was deconvoluted into 3 peaks in the wavenumber range from 350 to 1000 cm^{-1} and their assigned vibrational modes are summarized in Table 5. It can be seem that the band has shifted after the heat treatment. All the peaks at around ~466, ~669 and ~767 cm^{-1} which are chosen as A, B, and C bands respectively. Bands at around 466 cm^{-1} which are included as intermediate region of Raman scattering has generally been ascribed to the to the deformation vibration modes of glass network structure with bridged oxygen [27]. Those peaks are assigned to the symmetrical stretching or bending vibrations of Te-O-Te linkages. They are formed by corner sharing of (TeO_4), (TeO_{3+1}) polyhedral and TeO_3 units [28]. The peak observed in range 669 cm^{-1} may be assigned to the symmetrical stretching vibrational modes of $(Te_{ax} - O)_s$ of TeO_4 tbp units [28, 29]. The broad peaks observed at around 767 cm^{-1} are for the $(Te_{eq} - O)_s$ and $(Te_{eq} - O)_{as}$ vibrations modes of TeO_{3+1} or TeO_3 tp units [28, 30].

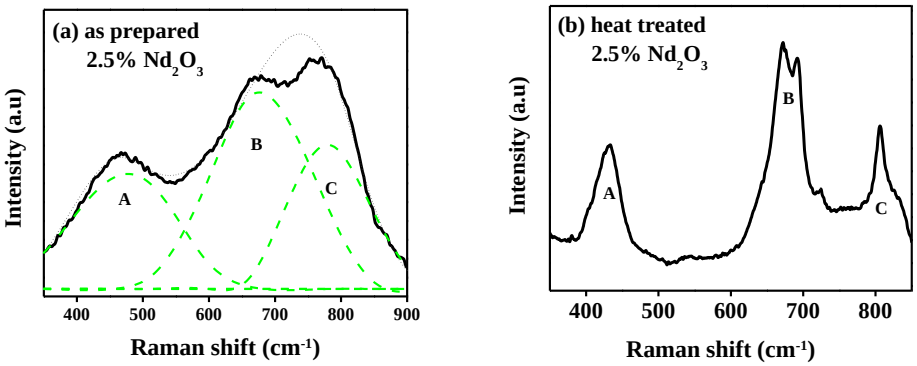

Fig.7: Raman spectra of $72.5TeO_2$-$15MgO$-$10Na_2O$-$2.5Nd_2O_3$ glass system (a) as prepared (b) heat-treated glasses.

Table 5: Raman peak positions of prepared and heat-treated samples.

Glass with 2.5% Nd_2O_3	Raman (cm^{-1})		
	A	**B**	**C**
As prepared	466 Te-O-Te	669 TeO_4	767 TeO_3/TeO_{3+1}
Heat-treated	433 δ-TeO_2	672 690 α-TeO_2	807 γ-TeO_2

Figure 7(b) shows three strong and sharp peaks around ~433, ~672, and 807 cm^{-1} and a weak peak at about 690 cm^{-1} which Raman assignments is listed in Table 5. Crystalline TeO_2 has two polymorphic forms of planes which are the tetragonal α-TeO_2 (paratellurite) [31] and the orthorhombic β-TeO_2 (Tellurite) [32]. However, Mirgorodsky et al. reported that crystalline phases are consist of α-TeO_2, γ-TeO_2, and δ-TeO_2 [33]. The band at 433 cm^{-1} is ascribed to δ-TeO_2 [34] and the Raman spectrum of α-TeO_2 contains bands at high intensity at 672 and 690 cm^{-1} at low intensity are assigned to symmetric stretching vibration of TeO_4 TBP. The high intensity of band at 672 cm^{-1} may because of the large difference in the polarizabilities of Te-$_{ax}$O and Te-$_{eq}$O bonds [35]. The last band at 807 cm^{-1} is attributed to vibrations modes of TeO_3 TP or TeO_{3+1}. Comparison of the intensities of each peak for as prepared $72.5TeO_2$-$15MgO$-$10Na_2O$-$2.5Nd_2O_3$ glass and the crystalline glass shows that the peak for heat-treated sample is higher. This is agreement with the result obtained by Di Bartolo [36] and Kabalci et al. [34]. These results indicate that the structural changes take place in the glass network after the heat treatment. This is due to existence of nanocrystals which contribute to the enhancement of local electric field which consequently increase the polarizability between the ions in the glass. The increase in polarizabilty with increase the intensity of Raman peaks.

Conclusions

The physical and structural properties of TeO_2-MgO-Na_2O glasses have been investigated as effect of Nd_2O_3 content heat treatment process. The properties of density, molar volume and ionic packing density were discussed with different Nd_2O_3 contents. It is found that Nd ions have entirely filled the space and make the glass more compact. The occurrence of crystallite particle was determined by TEM and it is observed that the average size is about ~8.30 nm. IR studies discovered that the incorporation of Nd_2O_3 in place of TeO_2 increased the number of non-bridging oxygens by gradually replacing TeO_4 (tbp) unit with TeO_3 (tp) through TeO_{3+1}. Raman results show that the glass network consists of TeO_3 and TeO_4 for glass whereas α-TeO_2, δ-TeO_2 and γ-TeO_2 for crystalline peaks.

Acknowledgments

The financial support from Ministry of Higher Education, RMC, UTM through the research grant (vote 4L657, 4F752, and 4F319) are highly appreciated.

References

[1] J.E. Stanworth,. Tellurite Glasses. Journal of Nature.**169,** 581 (1952).
[2] S., Suehara, K. Yamamoto, S. Hishita, T. Aizawa, S. Inoue, A. Nukui,. Bonding Nature in Tellurite Glasses. Physical Review B. **51** (21): 14919 (1995)
[3] R.A.H.,El-Mallawany, 2002: CRC Press, Boca Raton, Florida.
[4] R.A. Narayanan, J.W. Zwanziger, Journal of Non-Crystalline Solids. **316**(2-3), 273 (2003)
[5] G. Kaur, T. Komatsu, R.,Thangara, J. Mater. Sci. **35,** 903 (2000)
[6] R. Singh, J.S. Chakravarthi,. Physical Review B. **55**(9), 5550 (1997)
[7] M.A.P., Silva, Y. Messaddeq, V. Briois, M. Poulain, F. Villain, S.J.L. Ribeiro,. Journal of Physics and Chemistry of Solids.**63**(4): 605 (2002)
[8] A.P. Mirgorodsky, T. Merle-Mejean, J.C. Champarnaud, P. Thomas, B. Frit,.Journal of Physics and Chemistry of Solids. **61**(4): 501 (2000)
[9] S., Blanchandin, P. Thomas, P. Marchet, J.C. Champarnaud-Mesjard, B. Frit,. Journal of Alloys and Compounds. **347**(1-2), 206 (2002)
[10] R.T.,Shannon, Acta Crystallographica Section A: Crystal Physics, Diffraction, Theoretical and General Crystallography.**32** (5): 751 (1976)
[11] N.A.M.,Jan, M. Sahar, S.K. Ghoshal, R. Ariffin, M. Rohani, K. Hamzah, S. Ismail. Thermal and Photoluminescence Properties of Nd3+ Doped Tellurite Nanoglass. in Nano Hybrids. 2013: Trans Tech Publ.
[12] V.V.,Gowda, Physica B: Condensed Matter.**426**, 58 (2013).
[13] N. Yusoff, M. Sahar, Physica B: Condensed Matter.**456**, 191 (2015)
[14] B.V.R. Chowdari, P.P. Kumari, Solid State Ionics.**113**, 665 (1998)
[15] S. C.E., Rada, M. Rada, P.Pascuta, V. Maties, J. Matter Sci.**44,** 3235 (2009)
[16] H., Burger, K., Kneipp, H., Hobert, W. Vogel,. Journal Non Crystalline Solids. **151**, 134 (1992).
[17] L. Hu, Z. Jiang,. Physics and Chemistry of Glasses. **37**(1), 19 (1996)
[18] P.G., Pavani, K. Sadhana, V.C. Mouli, Physica B-Condensed Matter.**406**(6-7), 1242 (2011)
[19] N. Yusoff, M. Sahar, S. Ghoshal, Journal of Molecular Structure.**1079,** 167 (2015)
[20] V.,Nazabal, S.,Todoroki, A.,Nukui, T.,Matsumoto, S.,Suehara, T.,Hondo, T., Araki, S., Inoue, C., Rivero, T., Cardinal,. J. Non-Cryst. Solids.**325,** 85 (2003)
[21] R.C.,Lucacel, I. Marcus, I. Ardelean, O. Hulpus,The European Physical Journal Applied Physics.**51**(03), 30901 (2010)
[22] V., Kamalaker, G. Upender, M. Prasad, V.C. Mouli, Indian Journal of Pure & Applied Physics.**48**(10), 709 (2010)
[23] M.,Arnaudov, V.,Dimitrov, Y.Dimitriev, L.,Markova,. IR-spectral Investigation of Tellurites. Res. Bull.1121, 1982.
[24] I.,Shaltout, Journal of Materials Science.**35**(2), 323 (2000).
[25] Sharaf El-Deen, L.M., Al Salhi, M.S., Meawad, M. Elkholy., Journal of Alloys and Compounds.**465**, 333 (2008)
[26] S., Rada, A. Dehelean, E. Culea, Journal of molecular modeling.**17**(8), 2103 (2011)
[27] Takao Sekiya, N.M., Atsushi Ohtsuka and Mamoru Tonokawa,. Journal of Non-Crystalline Solids.**144**, 128 (1992)
[28] V., Kamalaker, G. Upender, C. Ramesh, V. Chandra Mouli, Spectrochimica Acta Part A: Molecular and Biomolecular Spectroscopy.**89**, 149 (2012)
[29] B.V.R.Chowdari, P.P. Kumari,. Raman spectroscopic study of ternary silver tellurite glasses. Materials Research Bulletin.**34**(2), 327 (1999)
[30] S.X.Shen, A. Jha, Raman spectroscopic and DTA studies of TeO(2)-ZnO-Na(2)O tellurite glasses. Glass - the Challenge for the 21st Century.**39-40**, 159 (2008)

[31] R.,El-Mallawany, Handbook of tellurite glasses, physical properties & data. 2002, CRC Press, Boca Raton, FL.
[32] P. Charton, P. Armand, Journal of Non-Crystalline Solids.**333**(3), 307 (2004)
[33] A. Mirgorodsky, T. Merle-Méjean, J.-C. Champarnaud, P. Thomas, B. Frit,. Journal of physics and chemistry of solids.**61**(4), 501 (2000)
[34] İ.,Kabalcı, G. Özen, M. Öveçoğlu, Journal of Raman Spectroscopy.**40**(3), 272 (2009)
[35] A., Santic, A. Mogus-Milankovic, K. Furic, M. Rajic-Linaric, C.S. Ray, D.E. Day,. Croatica Chemica Acta.**81**(4): 559 (2008)
[36] Di Bartolo, B. and O. Forte,2007: Ottavio Forte.